DOI: 10.17277/amt.2016.03.pp.032-047

The Nature and Multiscale Techniques for Characterizatoin of Mechanical Properties: from Nanostructured Materials to Single Macromolecules

Part III. Nanoindentation and Atomic Mechanisms of Local Plastic Deformation

(*Continued*)*

Yu.I. Golovin

Institute for Nanotechnologies and Nanomaterials, G.R. Derzhavin Tambov State University,
33, Internatsionalnaya St., Tambov, 392000, Russian Federation;
Faculty of Chemistry, M.V. Lomonosov Moscow State University,
1-3 Leninskiye Gory, Moscow, 119991, Russian Federation

Tel.: + 7 (4752) 53 26 8; +7 (495) 939-16-82; *E-mail:* golovin@tsu.tmb.ru; lunin@direction.chem.msu.ru

Abstract

Up-to-date techniques for characterization of mechanical properties of materials (including biological ones) at all scale levels: macro-, micro-, nano- and atomic-molecular ones are considered. Particular attention is paid to atomic mechanisms of transition from elastic to plastic deformation. It is shown that a decrease in the size of crystalline object or its structural elements leads to a decrease in the activation volume, which characterizes the sizes of plastic deformation carrier, up to a volume comparable with atomic/ionic volume. It means that carriers of plastic deformation in nanoobjects are predominantly individual atoms and/or their small-atomic-clusters. As the size of the object or the size of plastic deformation zone increase, dislocation mechanisms start to operate. In macrobodies the formation of large clusters of dislocations, twins, grain boundaries migration, pore formation, micro-cracks become dominant.

Keywords

Mechanical properties of nanostructured materials; nanoindentation; single molecule force spectroscopy; theoretical strength; size effects in mechanical properties; atomic mechanisms of plastic deformation in nanoscale

© Yu.I. Golovin, 2016

Local deformation

Local loading often referred to as point loading is widespread in nature and technology. It occurs in dry friction (in the interaction of contacting surface microasperities) under abrasive and erosive wear, in fine grinding in various mills and mechanical activators, mechanochemical synthesis, interaction of grains in deformed nanocrystalline materials, atomic force microscopy and contact interaction of macromolecules, creating static and moving electric contacts in micro/ nanoelectronics, etc.

A good physical model of the processes in real dynamic nanocontacts is material surface testing by a solid sharp probe (usually a diamond one) with well-attested tip geometry. As a result of application of a controlled microload (~ 1 nN–10 mN) it is immersed in the intended nanosized object area which can be considered 0-dimensional. Simultaneously, the deformation response of the material is continuously measured with high-resolution (~ 0.1 nm) (see Section IV).

The behavior of the material under local loading has a number of features compared to the uniform one, so let us discuss it in more detail. In contrast to uniaxial tension/ compression in a continuous indentation with a sharp indenter (often a pyramidal one), the depth and radius of the contact area change from the atomic to the macroscopic, and the volume of plastically deformed region increases 10^{12}–10^{18} fold. Thus, as a sharp indenter penetrates into the material, different levels of structural deformation are encompassed. As a result of such size scanning, each structural level with its own range of characteristic sizes will bring its own characteristics into scale effects. To a certain extent it is similar to the situation

* Part 1. No. 1, 2016.
Part 2. No. 2, 2016.

with the Big Bang in the Universe. In both cases, there is a singularity at the initial time, and then the process of expansion of the object starts to develop from the point, experiencing a change in various sizes and ages, the dynamics of which follows very different laws. An increase in the contact load beyond limit of elasticity causes plastic deformation the nature of which can vary dramatically with the growth in indentation sizes. Thus, continuous indentation size effects (ISEs) may have different nature under different loads and indentation sizes.

The specific character of the elastic-stress state under any real indenter pressed into by normal force P, (for example, with a pyramid having a rounded tip with radius R) is such that according to Hertz (elastic contact of the rounded tip with the surface) the maximum shear stresses $\tau_{max} \approx 0{,}5\ P/A_c$ occur at a depth $\sim 0{,}5R$ below the contact area (A_c – its area), and almost pure hydrostatic compression which prevents initiation and development of plastic deformation is realized in the near-surface layer. This leads to a decrease in the material yield strength sensitivity to the state of the sample surface at point loading.

The elastic limit in NI was studied for a wide range of crystalline, amorphous and polymeric materials (Cu, Al, Au, W, Nb, Fe, Zn, Ta, Ni_3Al, MgO, KCl, LiF, CaF_2, InPb, c-BN, 4H SiC, etc.) in a variety of test conditions [221–234]. It has been found that in many cases the elastic-plastic transition occurs unevenly and is accompanied by rapid immersion of the indenter into the material under constant load (Fig. 26). This phenomenon is similar in nature to sharp yield point which some single crystals (silica, ice, etc.) demonstrate when tested in a rigid Instron type machine.

Due to the development of NI technology and a series of carefully designed experiments, it was found that strain jumps in elastic-plastic transition are determined by the processes of homogeneous generation of dislocations in the region of high shear stresses under the indenter [221–223]. Direct in situ observations under a transmission electron microscope [224–227] and atomic modeling of elastic-plastic transition [221] confirmed and clarified these ideas. At the same time there evolved a theory originated from the "first" quantum-mechanical principles of analysis of the

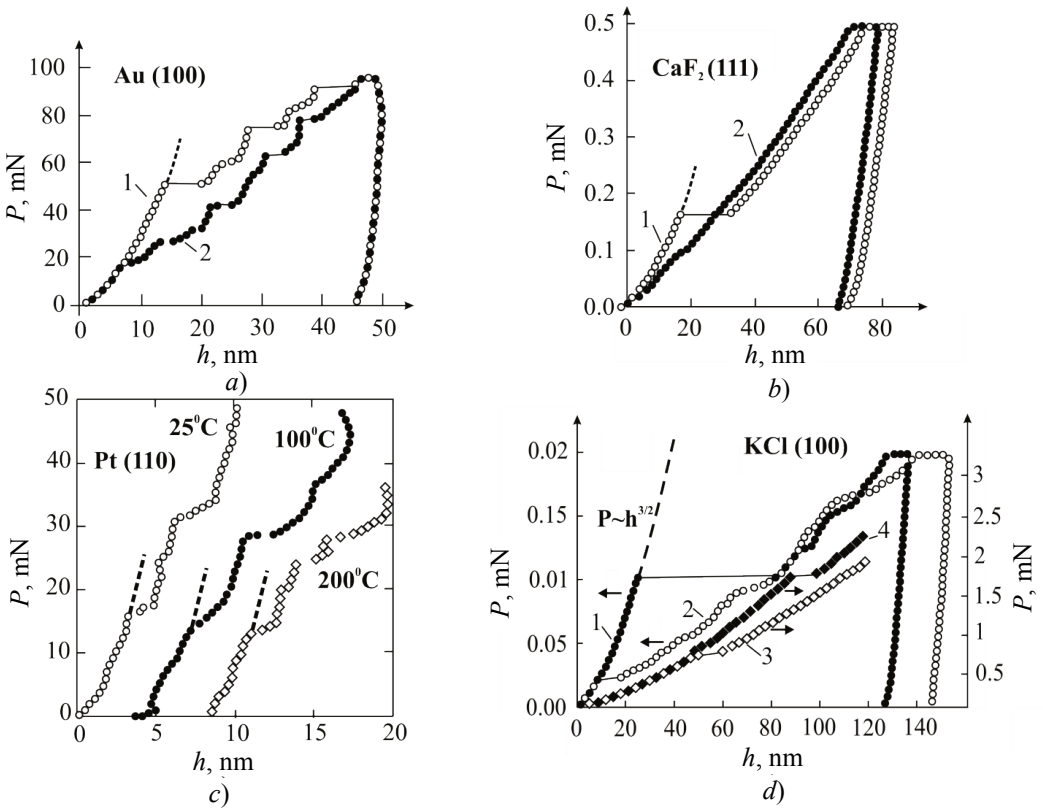

Fig. 26. *P-h*-diagrams for a number of crystalline materials at low loads
(experimental data are shown by dots, Hertz curve – by a dashed line):
a – single crystal gold (100), t = 20 °C: *1* – atomically smooth surface; *2* – indentation in the field of locating a step of about 2 nm high; *b* – single crystal fluorite (111), t = 20 °C: *1* – cleavage surface; *2* – surface after mechanical polishing; *c* – single crystal platinum (110); the surface was first polished mechanically and then electrochemically up to roughness height of less than 1 nm. The dependences obtained at different temperatures are shown next to the corresponding groups of points and artificially shifted by ~4 nm relative to each other for clarity; *d* – monocrystalline potassium chloride (001) – plane, t = 20 °C: *1*, *3*, *4* – smooth terrace on the cleavage surface; *2* – cleavage surface after mechanical polishing. Loading rate, $\dot{\varepsilon}$, s^{-1}: *1* и *2* – 1,75; 3 – $1{,}2 \cdot 10^4$; *4* – $1{,}7 \cdot 10^5$

crystal lattice resistance to mechanical stresses [221] and models of homogeneous generation of dislocations [222]. Application of thermal activation analysis played an important role in the analysis of atomic mechanisms of elementary plasticity [228–230, 235–243].

In the sub-micron and micron area of the indentation depth dependence $H(h)$ in the materials exhibiting ISE is typically well approximated by function of the form $H = Ih^{-i}$, where i ranges from 0.12 to 0.32 [244]. At homologous temperature $T_h < 0{,}3T_m$ (T_m – melting point) ISE begins to emerge only at $h < 10$–20 μm. Some metals with a high modulus of elasticity (W, Ir, and others) have sensitivity zone H to the indentation depth which extends up to $h \sim 100$ μm. Polycrystallinity and reduction in the grain size d, by contrast, leads to a shift of the border of the ISE initiation into the area $h \leq d$. Extrapolation of these dependencies to $h = a_0$ (where a_0 – a lattice parameter) gives value H which is close to the theoretical strength. It was shown above that at the initial penetration stages of a sharp indenter values $H \approx \tau_{th}$ are really realized. For amorphous materials ISE reveals itself weakly (if any exists). Several materials have nonlinear dependence $\lg H = f(\lg h)$ which can be approximated by two or more straight lines rectilinear sections (Fig. 27).

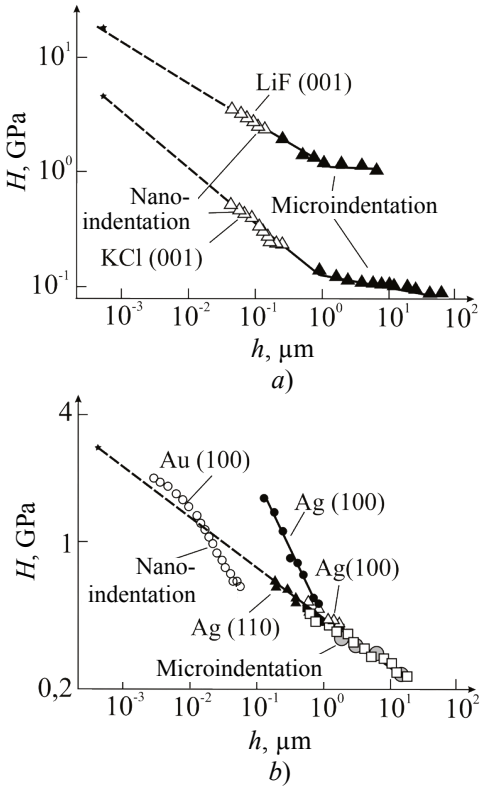

Fig. 27. Size dependences of hardness for some single-crystal materials
(different points correspond to different authors' data):
a – ionic crystals; *b* – metals [244]

There are quite a lot of assumptions regarding the nature of the ISE. However, there is not an accepted view on this issue. And it is unlikely to be reduced to a single model suitable for a wide range of materials and a variety of test conditions. What is clear is that NI size effects are related to structural aspects of constrained plastic deformation.

Biomaterials

Physical-mechanical properties of biomaterials (membranes, capillaries, blood vessels, bone and soft tissues, chitin integument, muscle fibers, etc.) are important for many vital processes – from detection, immobilization, proteins conformation change, peptides, enzymes up to expansion of capillary by passing blood cells, skeleton deformation while walking and muscle contraction. The functionality of various biological objects, kinetics, and the very capability of many processes is determined by stiffness, yield strength, strength, viscoelasticity, creep speed, viscoelastic recovery and other conventional mechanics characteristics. Their total or deviation from the norm can be a source of information on the state of biological objects or serve as diagnostic features. Modern metrology tools allow you to explore these characteristics at different scale levels – from macro- to nano-, including nanomechanical properties of single macromolecules.

Nanomechanical tests of biomaterials have their specific nature: as a rule, their results are strongly affected by temperature, humidity, composition of the surrounding atmosphere, etc. Therefore, they are usually tested in the climatic chambers. Another feature of the majority of biological objects is their low stiffness, which requires applying small loads and strain sensors with a large stroke. Finally, they are characterized by time-dependent behavior, which leads to a strong dependence of the properties on the rate and duration of load application. In this respect they are similar to synthetic polymers generally exhibiting viscoelastic behavior in mechanical tests.

There are a number of reviews and original articles devoted to biomechanical properties of biomaterials [245–259]. Let us demonstrate some approaches to nanomechanical testing of biomaterials and the most striking results by a few typical examples. For instance, practical guidance on the application of NI methods for the characterization of different biomaterials is given in [246], a review of the results obtained by these methods on hard mineralized tissues is presented in [257], and – on the soft tissues – in [258]. Methods for determining the viscoelastic properties and microstructure of single cells in a SEM column with simultaneous use of the nanoindenter and probes with both sharp and flat tips are described

in [259]. The changes in microstructure and mechanical properties of bone tissues in animals in the function of their age are discussed in [255], and due to sclerotic dentin affection in [256].

In general, we should note the rapid growth of the number of publications in the last 3–5 years on the use of nanomechanical testing of different biological tissues, materials and objects in biomedical research in order to monitor the body's condition and early diagnosis of diseases.

Atomic mechanisms of deformation and fracture in nanoscale

It should noted at once that, despite obvious progress in the understanding of atomic deformation and fracture mechanisms in nanoscale made in recent years, many fundamental questions remain debatable. An increase in sensitivity of nanomechanical devices and techniques, temporal and spatial resolution of electron microscopes, spectrometers, etc. enabled to get close to the spatial and temporal scales of elementary events in the dynamics of structural defects, but many of them are still outside the experimental capabilities. The processes of dislocation nucleation in various sources, their interaction with each other and various obstacles, not to mention the dynamics of point defects with even smaller scale, are not available for direct observation. The highest achievement is the registration of the nucleation of individual dislocation loops in situ in an electron microscope column by a picoindenter set in it [83–85]. The spatial resolution in video filming was ~1 nm, and a temporal ~1 s. When registering the loading chart, it was about an order of magnitude better. So far it does not allow observing the dynamics of elementary acts of dislocations at the atomic scale of displacements and times, and registers only the sum total of a small number of such events. Therefore, the information about the elementary plasticity processes details has still to be removed from the indirect evidence and results of computer simulation.

Thermoactivation analysis

As with chemical macrokinetics, considerable progress in understanding the mechanisms of plastic flow and fracture can be achieved using thermal activation (**TA**) analysis of experimental data. Usually this is done using the modified Arrhenius relations, which being applied to the problems of nano-/micromechanics of materials are called S.N. Zhurkov's formulas. For example, for plastic flow rate we take

$$\dot{\varepsilon}_p = \dot{\varepsilon}_0 \exp\left(-\frac{U_0 - \gamma\sigma}{kT}\right), \qquad (10)$$

where U_0 – activation energy; γ – activation volume; $\dot{\varepsilon}_p = \dot{\varepsilon} - \dot{\varepsilon}_e$ – rate of relative plastic deformation equal to the rate difference of the total $\dot{\varepsilon}$ and elastic $\dot{\varepsilon}_e$ deformation. Value U_o for all materials and deformation mechanisms can range from a few tenths to a few electron-volt units. Low accuracy with which U_o can be determined by NI methods (at its best about ten percent) is difficult to use to identify the atomic deformation mechanisms. On the contrary, value γ for different mechanisms varies in a very wide range (Fig. 28) – from tenths of atomic volume a_o

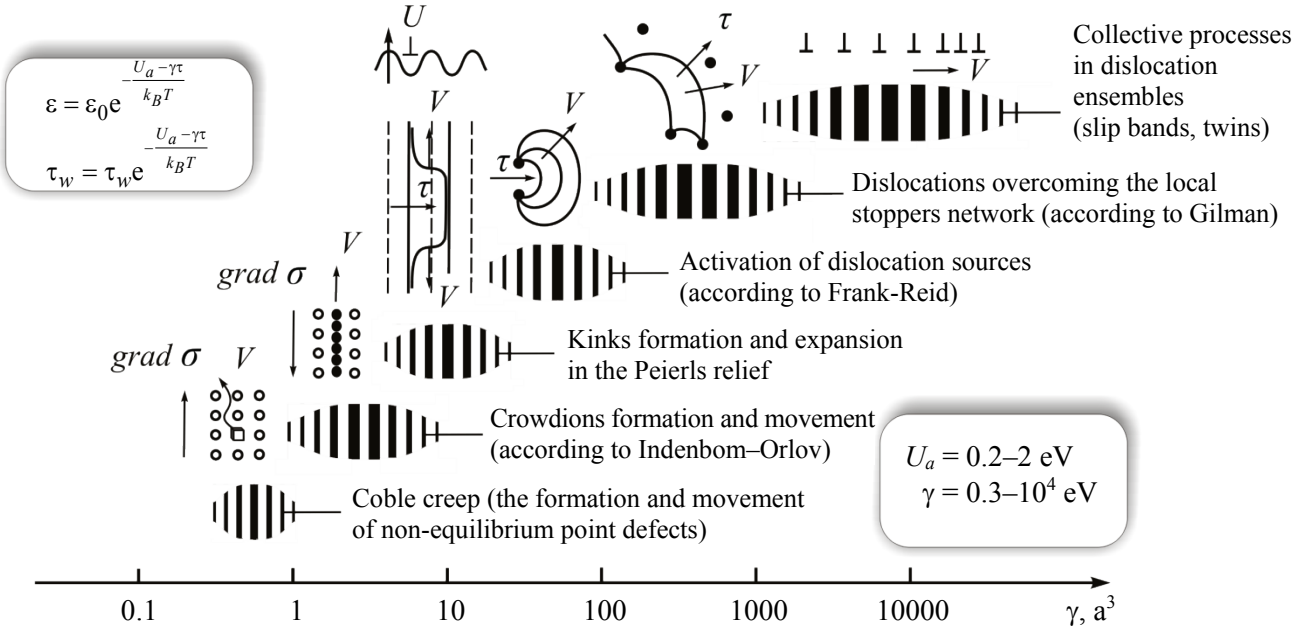

Fig. 28. Schematic representation of different atomic mechanisms of plastic deformation and ranges of values of their activation volume

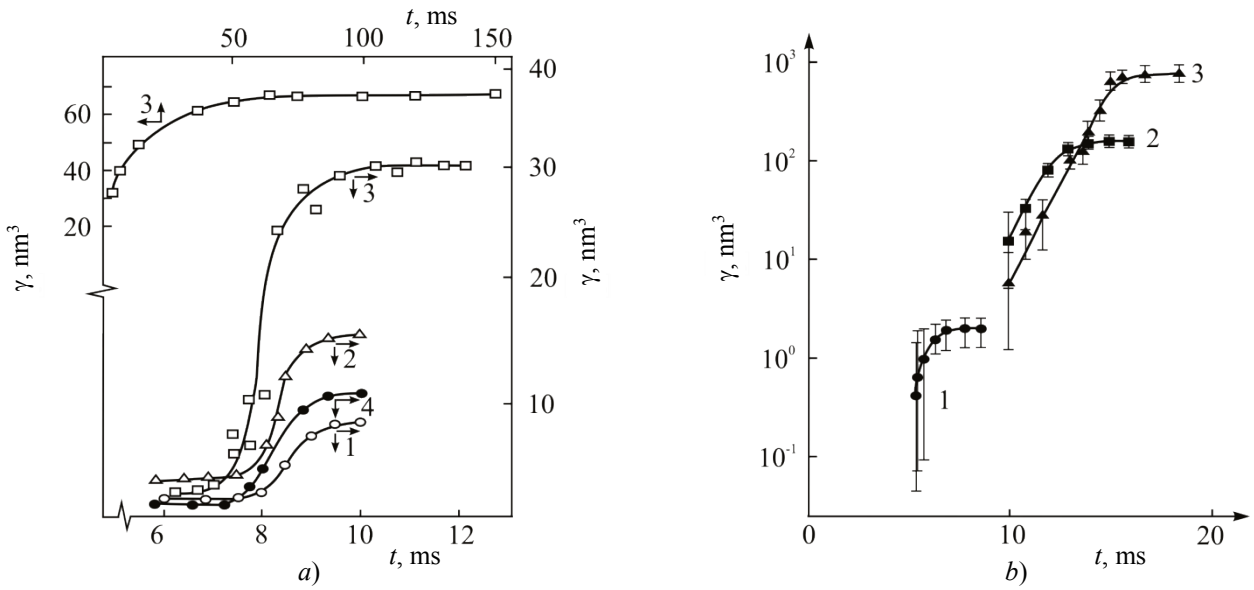

Fig. 29. Kinetics of the activation volume change as an indenter immerses deeper in a variety of materials: *a* – ionic crystals; *b* – metals

(for migration of individual atoms) to many thousands a_o (for conservative dislocation clustering). This enables the identification of dominating mechanisms of plastic flow (or mass transfer), even if the accuracy of γ is determined only by the order of magnitude.

In [228–230, 237–243] according to the results of the experiments with "rectangular" power pulse loading (pulse duration in front ~5 ms, the relative deformation rate at the initial stage of indenter penetration ~10^3 s^{-1}), value γ, characterizing the type of the carrier and the atomic mechanism of plastic flow in single crystals of NaCl, LiF, MgO, Al, Pb, $Co_{50}Fe_{35}B_{15}$ amorphous alloy and other materials, was measured. For all the studied materials γ turned out to be of the same order as atomic volume a_o at the early stages of rapid indentation (Fig. 29), and only at the later stages and greater depths, it was getting equal to tens – hundreds of atomic volumes [238–242]. This clearly indicates a lack of self-similarity of indentation process and the leading role of point defects and their small-atomic clusters (probably, crowdions – condensations of linear density of atoms along the close-packed directions in a crystal) in mass transfer at the initial stages of rapid indenter penetration and initiation of dislocation mechanisms of flow in subsequent stages. Similar results were obtained in these studies using another method – on the kinetics of the electric polarization of ionic crystals under the indenter [228].

In [241–243] the contribution of dislocation mechanisms in general plastic deformation under these conditions was estimated. As the dominant flow mechanism changed this share dropped from 100 to a few per cent in plastic crystals.

The nature of first jumps of plastic deformation

In their fundamental works [221, 222] a group of renowned experts in nanomaterials science from MIT (USA) reviewed the literature on the nature of the initial jumps of deformation under NI in FCC single crystals of Al, Cu, Au, Ir and presented their own results obtained experimentally, theoretically and using computer modeling. In these studies from the first principles the energy criterion of elastic stability loss of the crystal lattice was deduced. It is based on the analysis of soft phonon modes in a lattice of a given symmetry and allows us to predict the conditions of homogeneous nucleation of a dislocation loop or a twin, as well as their crystallographic characteristics. Using methods of 3D molecular dynamics the simulation of homogeneous nucleation of atomic defects in a cluster of about ~10^6 particles was performed. The results obtained are qualitatively consistent with the literature and the authors' own data obtained on single Al crystals.

In a series of studies of another group of scientists also from MIT [223, 231–234] the statistics of deformation jumps in 4H SiC and high purity (99.999 %) platinum with orientation (110) was carefully analyzed and thermal activation analysis was performed. It was established that when testing 4HSiC with an indenter having a tip radius R = 145 nm, value $\gamma = 4{,}6 \cdot 10^{-3}$ nm^3, while for the indenter with R = 300 nm, $\gamma = 2{,}3 \cdot 10^{-3}$ nm^3. For Pt $\gamma = (9{,}7 \pm 1{,}9) 10^{-3}$ nm^3 was found.

In another extremely interesting paper [260] a similar method was used to investigate the dependence

of waiting time of the first jump of deformation in intermetallic Ni_3Al (the initial dislocation density of 10^5 sm^{-2}) on the value of subcritical load P_S on the indenter. In contrast to [222, 228, 230], the load on the indenter did not increase linearly with time but was fixed at a subcritical level. The critical load value P_c was previously determined at a low rate of increase in indentation force. This formulation of the experiments made it possible to accumulate extensive jumps statistics, which allowed, in turn, a more thorough analysis of their nature.

As expected, a decrease in P_S led to an increase in the average waiting time and its dispersion, i.e. dislocation nucleation process was of a thermally activated character. When homogeneous nucleation of dislocation loops in dislocation-free areas occurs absolutely at random (where the indenter was with a probability very close to unity, with the average distance between the growth dislocations > 20 μm and the indentation diameter ~ 100 nm), the differential distribution of jump waiting time must follow the exponential law. As in [222], such a distribution pattern was actually observed, but only under pre-critical load P_S = 500 μN (Fig. 30 *d*). This made it possible to estimate the activation volume γ. For Al and Ni it was about 0.02 nm^3. This fact suggests that the rate of loops formation in pure homogeneous nucleation was determined by small-atomic mechanisms.

At lower P_S (from 300 to 400 μN) the distribution of waiting times had maximum, the position of which depended on the value of P_S (Fig. 30 *a* – *c*). This testifies to the non-random nature of the process of

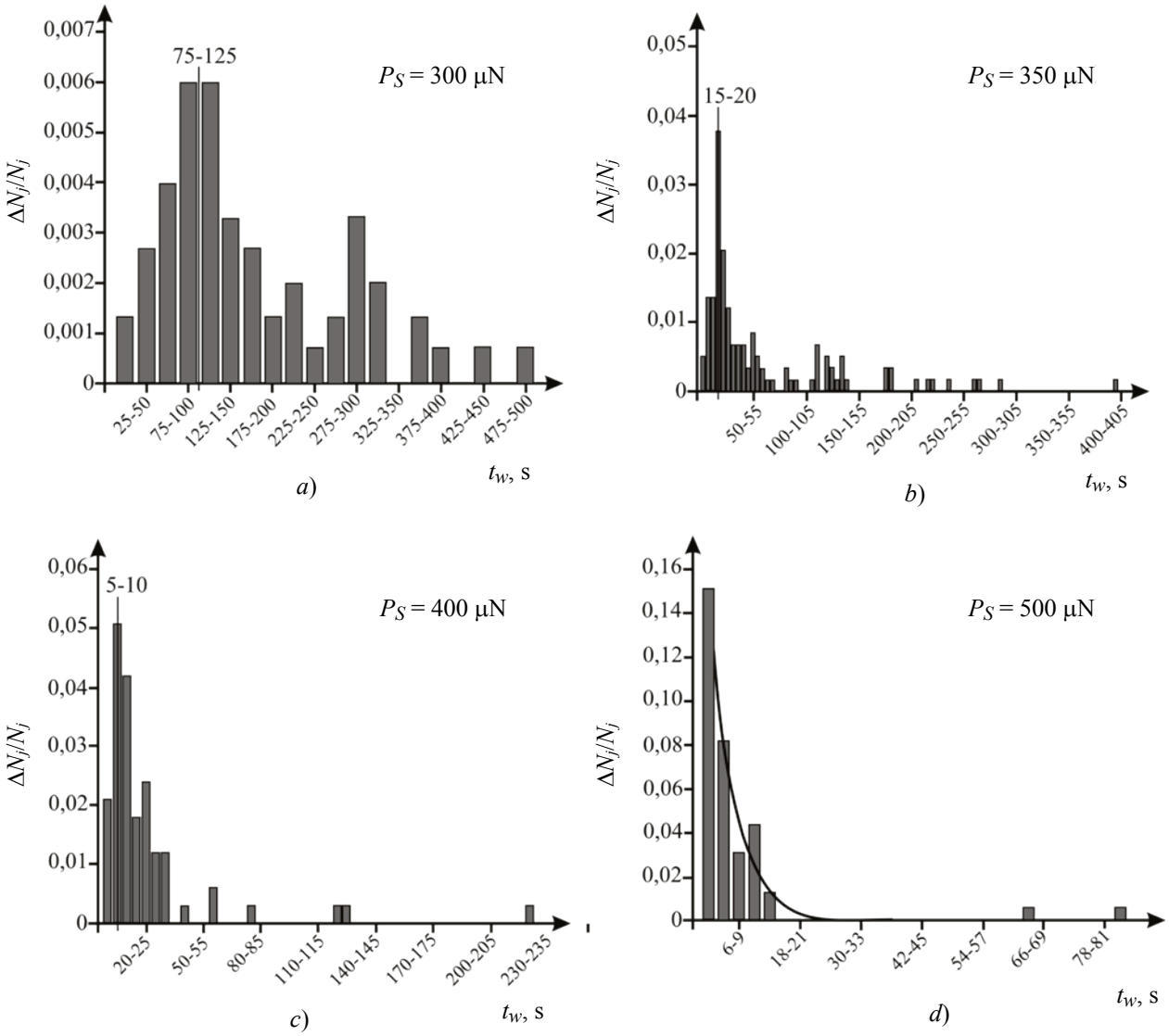

Fig. 30. Histograms of jump waiting time under four different loads:
a – P_S = 300 μN, N_j = 60; *b* – P_S = 350 μN, N_j = 117; *c* – P_S = 400 μN, N_j = 67; *d* – P_S = 500 μN, N_j = 53
(solid line in *d*) – approximation exponent. N_j – the total number of jumps at a given load P_S [260])

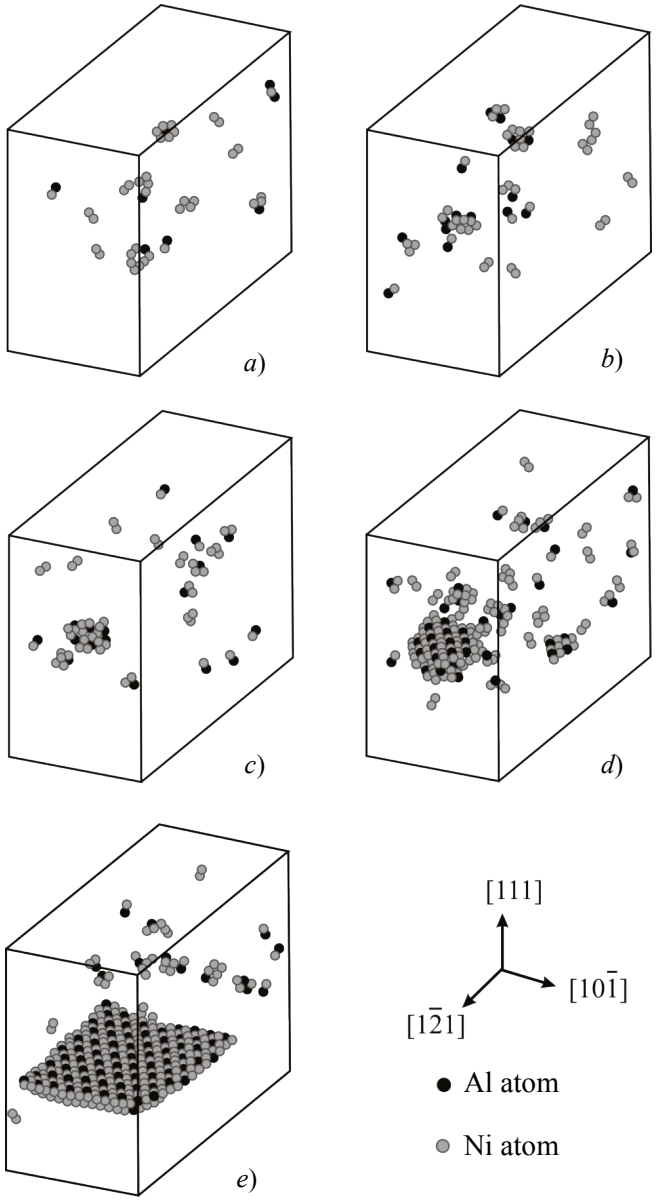

Fig. 31. The results of modeling the nucleation defects under constant shear stresses applied along [101] by methods of molecular dynamics (only those atoms are shown which are displaced from their points at distances of about a few tenths of the lattice parameter)

loops nucleation, which has some prehistory. The authors consider small-atomic clusters containing a few Ni and Al atoms as dislocation precursors. They call them "hot spots" in the volume of a crystal. Modeling by molecular dynamics method with the interaction potential proposed in [260] showed that, indeed, Shockley partial dislocations nucleate in places where short-lived ($\sim 0{,}6 \cdot 10^{-13}$ c) clusters of strongly displaced Ni and Al atoms are pre-generated (Fig. 31). This leads to the emergence of the prehistory in "homogeneous" nucleation of dislocation loops, which ceases to obey an exponential distribution of delay times. The rate of their generation $\dot{N}$ under any load (except for $P_S = 500$ μN) increases exponentially with the exposure time, which means linear in time fall in the activation energy. This result is consistent with the assumption that atomic scale damage under load accumulates. At $P_S = 500$ μN or higher the size of precursors required for loop nucleation becomes atomic and no longer limits the rate of their generation, therefore their nucleation occurs completely at random and purely homogeneously.

Homogeneous nucleation of dislocations under the indenter

As follows from the preceding paragraph, among all possible causes of the formation of large jumps under small local loads ($P \leq 1$ mN)) the most likely one is the nucleation and expansion of dislocation loops. In well-annealed crystals the average dislocation density ρ can be 10^4–10^6 sm^{-2} which corresponds to the average distance between them 10–100 μm. Approximately the same is the range of grain sizes d in conventional polycrystalline materials. This is several orders of magnitude higher than the deformation zone size during nanoindentation with a sharp indenter at $h_c < 100$ nm. Therefore, with high probability (in annealed crystals it is very close to unity) the indenter indentation takes place in the dislocation-free area, away from grain boundaries, i.e. virtually – in a perfect single crystal. In other words, theoretical strength can be realized in nanocontact interaction that should be taken into consideration when designing nanomechanical products and tools to make them.

In [52] models of homogeneous nucleation of dislocation loops under the indenter are presented. The model in [261] takes into account that for the occurrence of the first loop it is necessary to achieve not only the critical shear stress, but also a highly stressed area of a certain size under the indenter, exceeding the critical size of the loop.

The possible role of point defects

The role of small-atomic clusters of intrinsic point defects as precursors in the homogeneous nucleation of dislocations was discussed above. Let us now consider the possibility nondislocation plasticity mechanisms, realized through diffusion and migration mobility of nonequilibrium point defects. Usually it is considered to be effective only under the creep at high temperatures ($T \geq 0{,}5\ T_m$, где T_m – melting temperature) and low applied stresses σ. In the annealed single

crystals and coarse polycrystals where grain boundary and pipe diffusion can be neglected, a decisive contribution to creep rate $\dot{\varepsilon}_{cr}$ is provided by volume diffusion through the grain body. It follows Herring-Nabarro law [262] which can be written in the Arrhenius form

$$\dot{\varepsilon}_{cr} = \frac{32a^3\sigma D}{\pi d^2 kT} = \frac{32a^3\sigma}{\pi d^2 kT}\exp\left(-\frac{Q}{kT}\right), \qquad (11)$$

where a – interatomic distance; D and Q – factor and energy of volume diffusion activation, respectively; d – sample size (or grain). The normal macroscopic deformation rate range according to this mechanism $\dot{\varepsilon} = 10^{-10}$–$10^{-5}$ s^{-1}.

As already noted, at the initial stages the pyramidal indenter penetrates into virtually dislocation-free area of the annealed crystal. Grain boundaries (if any) are at a great distance and can not participate in the deformation. Thus, the applicability conditions (11) are met. Now pay your attention to the fact that in (11) the characteristic size of problem d is in the denominator in the second degree. This means that when the object scale decreases from macro ($d \sim$ 1–10 mm) to nano ($d \sim$ 10–100 nm), the rate of plastic flow according to this mechanism can increase about ~10^8–10^{10} fold. Stress σ before the elastic-plastic transition reaches ~0,1 E, which is several orders of magnitude higher than the values normal for creep. Substituting in (11) the numerical values $\sigma = 0{,}1\,E$, $d \approx$ 10–100 nm and typical values of D or Q for solids at $T \approx$ 300 K it is easy to get convinced that, in principle, such a mechanism can provide plastic deformation at a rate of $\dot{\varepsilon} \approx 10^1$–$10^4$ s^{-1}.

Under the creep it is vacancies that are considered to the main carrier of plastic deformation. The authors of [263, 264] proposed and justified the mechanism of flow, which is realized under conditions of high pressure and stress gradients due to the generation and movement of interstitial atoms along the close-packed directions.

Using methods of molecular dynamics it was established [265–267], that even in the "soft" FCC crystals (Cu, Ni, Fe) originally small-atomic clusters of point defects form, which can move themselves under the action of applied stresses, or from which dislocation loops may subsequently develop [265, 266]. In the latter case, the clusters of point defects act as precursors for dislocations, just as is the case with radiation damage to the crystals. Energy considerations applied in [267] to calculate the stability of such clusters of interstitial atoms show that with increasing number of atoms N in them (to a certain moment) the energy normalized to N falls making such "condensations" more likely than the appearance of single interstitial atoms. At the same time by merging quasi-crowdions in planes (110) the clusters form by the way of single- or double-layer "pancakes" (Fig. 32). They may subsequently become nucleation centers of dislocation loops of a critical size (for a given stress level).

Note that in order to explain dependence $H(h)$ in the submicron region a number of researchers used the theory of gradient plastic deformation [268–272], whose foundations were laid in [273]. But it is no longer consistent with the experiment for $h \lesssim 100$ nm. With such small h it predicts unrealistically high dislocation density (> 10^{14} sm^{-2}) and unlimited growth of H with a further decrease in h. Moreover, it is well known that in nanoscale objects (nanoparticles, nanofilms, nanoindentations with characteristic sizes $R^* < 50$–100 nm) the nucleation of dislocations becomes difficult, and at even smaller sizes – it becomes

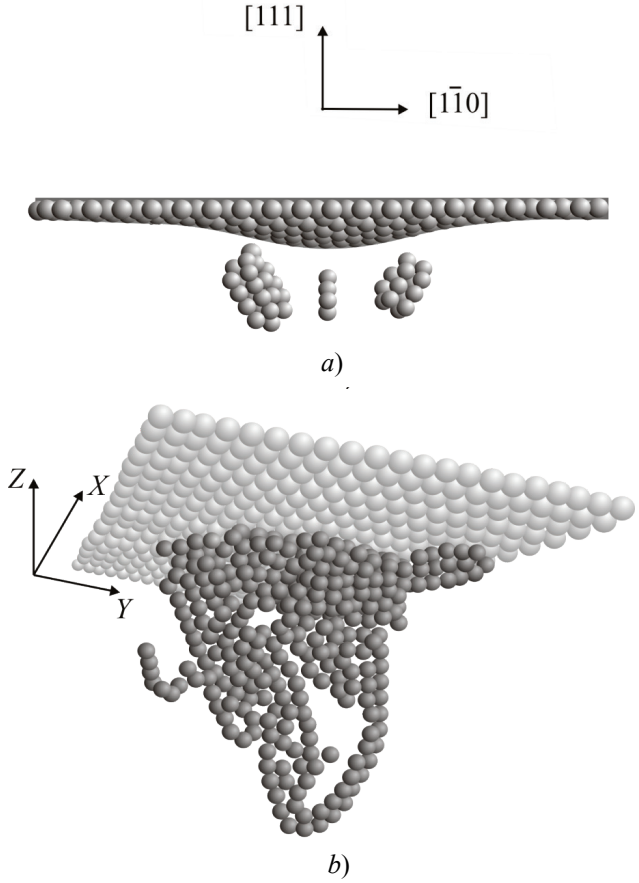

Fig. 32. The results of modeling the initial stage of plastic deformation under the indenter by methods of molecular dynamics [267]:
a – nucleation of clusters of point defects;
b – nucleation of the first dislocation loops.
Modeling pictures show only those atoms which displaced from the lattice points by the amount of more than ~0.2 from the interplanar distance

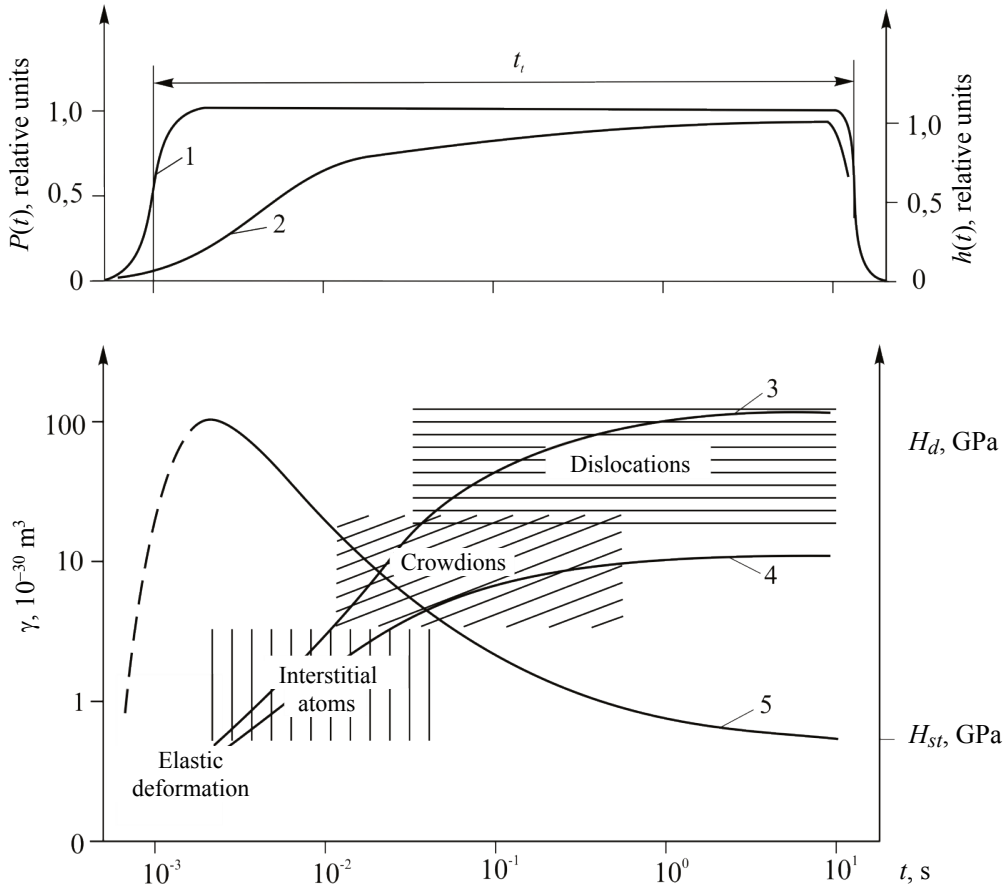

Fig. 33. The scheme of deformation mechanisms change under dynamic nanoindentation:
1 – indentation force $P(t)$; *2* – indentation depth $h(t)$; *3* – activation volume γ for soft materials (Pb, NaCl, LiF); *4* – activation volume γ for hard materials (Si, amorphous metal alloy $Co_xFe_yB_z$); *5* – dynamic microhardness H_d; H_{st} – quasistatic hardness. The dashed line denotes the dependence of the mean contact stresses at the initial elastic portion of the indenter penetration into the material

completely impossible due to the strong growth of necessary stresses. For example, for a Frank-Read source they reach the theoretical shear strength at $R^* \leq 10$–20 nm (according to $\tau \approx 2\pi Gb/R^*$). Moreover, critical stresses should be achieved in the region with critical sizes of the emerging loops rather than at a single point Consequently, the maximum stresses in the center of this region should be still higher than in the case of a uniform stress field.

To sum up, we would like to emphasize that all of the above data, obtained by independent techniques in different laboratories around the world, testify to a strong dependence of the atomic mechanisms of plastic deformation on the size of the locally loaded area. With increasing this area some modes of plastic flow are replaced by others (Fig. 33), whereby the mechanical properties under strong changes. In other words, it is a change of deformation mechanism that is of the main causes of SE in the mechanical properties of materials.

Mechanically Induced Phase Transformations

High mechanical stresses and pressure (particularly under dynamic nanocontact interaction accompanying fine grinding, abrasion wear, AFM probe effect on the surface of tested or modified material and others) can induce phase transformations in the solid. Due to this fact, an alternative channel of relaxation of elastic energy that competes with plastic deformation and fracture is implemented. At the same time both the density, elastic moduli, hardness of the material and deformation mechanisms change. Thermodynamic conditions and kinetics of phase transformation (**PT**) are very sensitive to the size factors, so we can expect significant changes in the phase diagram of the material in nanoscale. Herewith it is necessary to distinguish between two types of effects: a) the formation of new equilibrium phases under the applied load (these PTs may be reversible, i.e. a new phase

may disappear after unloading, or irreversible, i.e. it may be partially or fully preserved in a metastable condition after unloading) and b) stimulation of metastable phases relaxation and their transformation into more stable ones. The first type of PT includes the formation of high-pressure phases in the single-crystal silicon, ice, etc., which can be partially preserved after unloading [274]. Examples of the second type of PT are diamond graphitization under the indenter, the formation of nanocrysrals under amorphous alloys indentation [275, 276], the transformation of the tetragonal phase into the monoclinic one in ZrO_2 ceramics, resulting in a reduction of their fragility (transformation toughening) [277, 278].

It is clear that a decrease in the size of a grain, a single phase, a twin layer, etc. into nanoregion can significantly change the condition for the phase existence, nucleation mechanisms of these new phases, PT kinetics, the extent of the direct and inverse transformation and others. There are numerous data obtained mostly by NI techniques, testifying to the presence of strong SE in PT in nanomaterials and locally loaded macrosamples [279, 280]. They imply that size factors should be taken into consideration when analyzing the mechanisms of deformation and fracture of materials capable of undergoing PT under mechanical effect.

Fracture and crack resistance

Crack nucleation, slow subcritical crack growth and rapid supercritical crack growth are high stress relaxation processes which are alternative or additional with respect to the above discussed mechanisms of relaxation of elastic energy in the loaded area.

To evaluate the crack resistance a variety of ways have been developed. In particular, fracture mechanics proposes to use critical stress intensity factor K_{1c} [281, 282] as a measure of resistance to quasibrittle fracture. In a broader context the term fracture toughness (**FT**) is often used, which does not imply a specific technique for determining this value, but includes concept K_{1c}. In addition the concepts of impact strength A_p, ultimate strain ε_{max} and other energy characteristics of the material are used.

For the experimental determination of K_{1c} a sample of a standardized size and shape with a previously introduced crack of a given length is tested for uniaxial tensile or bending, bringing it to a complete fracture. The value of critical stress σ_c corresponding to the initiation of the crack with length l determines K_{1c} ($K_{1c} = k_f \sigma_c \sqrt{l}$, where k_f – a dimensionless coefficient that depends on the specimen geometry and loading scheme). These techniques are included in the national standards of almost all industrialized countries (see e.g. [283] in the Russian Federation), and the results obtained are repeatedly described in the literature (with regard to testing of ceramics, see e.g. [284, 285]). It should be noted that the implementation of these tests requires a large number of specially prepared samples of macroscopic sizes with an induced crack that predetermines their high material and labor input. In addition, they are not suitable for testing small quantities of substances, samples and components of submillimeter section, which are characteristic of modern instrumentation, MEMS/NEMS, etc. Therefore the replacement of standard techniques by more simple means of characterizing the crack resistance, suitable for testing micro-and nanoscale samples is highly desirable.

One of the possible ways is to use NI to bring the material into the local fracture. As with all other testing techniques using local loading, the determination of fracture resistance in this way is characterized by simplicity, rapidity, low cost and does not require specially prepared samples. At the same time a single sample or real part can be used to carry out multiple tests and find out statistical regularities of a fracture [286–290]. The latter are generally consistent with Weibull statistical theory of fracture [291]. Due to simplicity and accessibility these techniques are widely used in engineering practice. There are several detailed reviews [292–294] summarizing the results of the application of these techniques and empirical design formulas for evaluating fracture resistance of ceramics, glass, high-strength alloys, etc. A number of recommendations for conducting such tests have been made [293].

In [294] it is noted that if these recommendations are followed, the difference between K_c and K_{1c} values determined by conventional techniques usually does not exceed 30 % and within the same class of materials – 15 %. Perhaps, this accuracy is not sufficient for absolute measurements, but it allows ranking the materials according to crack resistance and, as a rule, it provides the same ranking order as the traditional techniques. Moreover, indentation allows for a relative measurement of FT variations when you change the mode of obtaining and processing of the same material, or related materials.

Since the processes of plastic flow and fracture are related (and often mutually dependent) you can also expect specific size effects in submicron- and

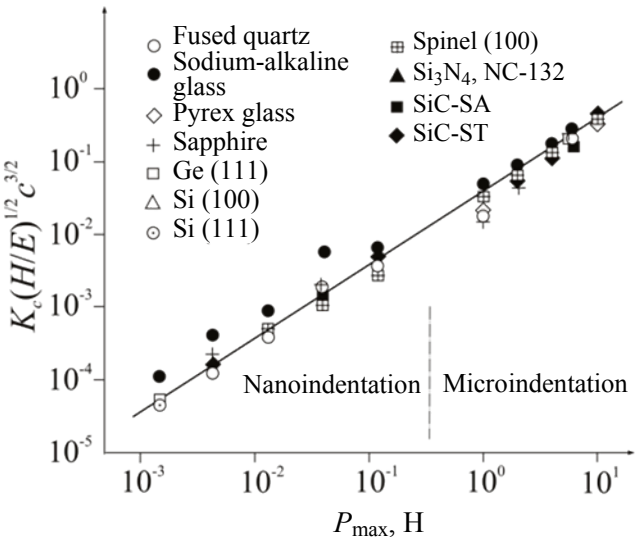

Fig. 34. Dependence of normalized crack length c on peak load P_{max} under indentation for a number of materials

nanoregion of the latter. It is obvious that the suppression of dislocation plasticity at $R^* \leq 100$ nm can lead to blocking the dislocation mechanisms of crack initiation. Indeed, when the indentation size is reduced, the geometric similarity between its depth and the length of the associated cracks ceases to be satisfied, and at certain critical depth (indentation strength) the cracks cease to arise even in brittle materials. In other words, stress localization in a smaller area leads to an increased plasticity role and reduction of the possibility of fracture to virtually zero. This is a useful effect which helps to create reliable silicon-based MEMS/NEMS, cantilevers and AFM probes, sliding pairs for microdevices, etc. There are currently a very limited number of published works dedicated to K_c determination under these conditions. Some of the most demonstrative results obtained are presented below.

In [295] critical force P_c needed for crack initiation under the Berkovich indenter was compared to that under the sharper "cube corner" indenter. It was established that in the second case P_c is from 10 to 1000 times less than in the first case. It is also important to understand whether the formulas which estimate K_c hold true with a strong decrease in P, resulting in a transition from macro- to micro, and then – to nanoindentation. In [295] there was examined the validity of

$$K_c = \alpha_i \left(E/H\right)^{1/2} \left(P/c^{3/2}\right), \qquad (12)$$

which was originally proposed in [281] for micro- and macro-scale testing by Vickers indenter, with a change in P by 4 orders of magnitude and using the "cube corner" indenter. From the results shown in Fig. 34 and 35 it follows that for all the investigated materials (see Fig. 34) scaling is preserved, and coefficient α_i in formula (12) is equal to 0.036. Figure 35 shows the interrelation between value K_c, obtained by indentation technique (indenter is a "cube corner", P varied from 1 to 100 mN), and K_{1c} measured by a conventional technique – by destructing prismatic samples notched according to a three-point bending scheme. From the data shown in this figure, it follows that values K_c и K_{1c} agree with an accuracy of ±40 %.

Thus, the validity of the application of NI techniques and calculation formulas of type (12) to estimate K_c, when load P decreases to at least 1 mN, was experimentally confirmed. They correspond to sizes R^* of the deformed region of tens to hundreds of nanometers in various materials. However, systematic studies of K_c dependence on R^* have not been carried out yet, and there are not any data on even smaller loads [295].

Dry friction

It is well known that true contact surface in friction pair is much smaller than the apparent one (typically 10–10^4 times less), and local pressure at discrete contact points is as many times higher than the apparent average value, respectively Friction force is considerably affected by deformation and fracture mechanisms of contacting asperities, as well as the nature and force of the atomic-molecular interaction at their interface. The large array of data obtained show

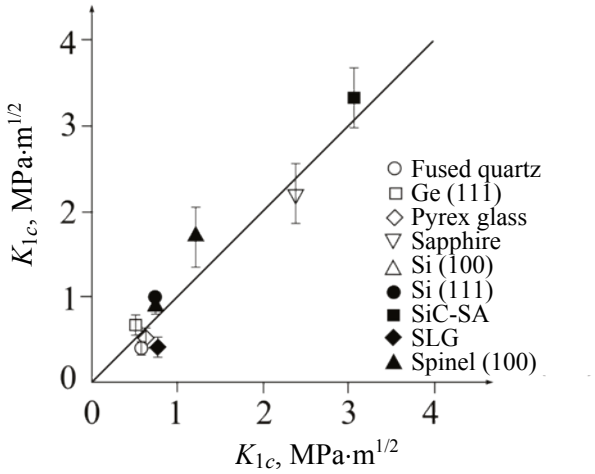

Fig. 35. The interrelation between fracture toughness measured by the traditional technique of three-point bending of notched prismatic samples K_{1c} and indentation by a cube corner K_c for a number of materials [295]

that the adhesion, plastic deformation and fracture in point contacts with different types of interaction are greatly influenced by size factors.

The intention to clarify the fundamental mechanisms of tribological phenomena led to the need for their study in nanoscale and atomic-molecular level.

Another manifestation of the SE in nanotribology is a reduction in local overheating caused by relaxation of elastic energy in contacting nanoasperities. Indeed, all other things being equal, the rate of heat release during plastic deformation $q \sim d\varepsilon/dt \sim v/R^*$ and the rate of temperature decrease due to heat conduction $\partial T/\partial t \sim \varkappa(R^*)^2$ (here v is linear rate of the relative displacement of surfaces, $\varkappa$ is thermal diffusivity coefficient of the material). In other words, heat removal from locally deformed areas into surrounding cold material volume improves with a decrease in roughness sizes as $1/R^*$. As a result, the amplitude of temperature flashes in plastically deformable asperities decreases with decreasing R^*.

Dry friction at the atomic scale

A number of materials (pure single crystal metals, ionic crystals, highly oriented pyrolytic graphite, MoS_2, and others) were used to achieve atomic resolution in the registration of friction forces when the probe of the atomic force microscope (in the lateral force registration mode) moves along the surface [2, 282]. When normal load increases the hysteresis (i.e. energy dissipation) also increases, which is consistent with increasing macroscopic friction force. The absolute values of the lateral force during the atomic friction are nevertheless remain considerably lower than those during the microscopic (non-atomic) friction, and friction coefficients can vary by more than an order of magnitude (Table 3). This effect is explained by the formation and sliding along the interface the contacting nanoasperities of edge dislocations like their sliding in the crystal volume. This can greatly facilitate and reduce shear friction coefficient f [297].

Quantum theory predicts that at a certain critical size of the contact spot and sliding conditions the friction should drop to zero, i.e. the mode of dissipation-free movement of the body on the surface of another body is realized (similar to the phenomena of superconductivity in electromigration or superfluidity in quantum fluid). The fundamental physical basis for this are the following considerations. For two atomically smooth surfaces sliding relative to each other the basic mechanism of energy dissipation is to convert the kinetic energy of the collective translational motion of atoms in the moving body into vibrational modes of the atoms of both interacting bodies. In an infinite solid the phonon spectrum has a continuous character. Thanks to anharmonicities one mode can be easily transformed into another under such conditions. As you reduce the size of the bodies and the area of their contact interaction the phonon spectrum becomes more and more discrete. Now, only certain combinations of modes can lead to dissipation of energy, and at a certain critical object size, the energy dissipation becomes impossible.

The experiment shows that under some scanning conditions the complete movement reversibility and the average value of the friction force equal to zero can be achieved [2]. However, this is possible only in a very specific situation when the forces of attraction (adhesion) are compensated by applying to the probe the equal force of the opposite sign (i.e. the force which tears off the probe from the surface) and slide instability is suppressed (like stick-slip). (The main reason for energy dissipation is strong motion nonuniformity of individual atoms belonging to two contacting surfaces).

To get rid of "sticking" and subsequent jumps it was proposed to "dismatch" the crystallographic directions in the interacting layers and thus eliminate spasmodic movements. Such a mode could be implemented in a specially designed atomic force microscope. By turning the graphite flakes, captured the probe, it is possible to pick up such disorientations with respect to the surface of the graphite sample, which lead to the disappearance of jumps and energy dissipation [2]. Such interaction and sliding mode are called structural lubrication or superlubrication.

Wear

The quantitative theories of wear which allow relating the macroscopic wear rate with the geometric and physical characteristics of the surface began to

Table 3

Friction coefficients for three materials under micro- and nanoscale testing [2]

Material	Root-mean-square height of roughness, nm	Friction coefficient in probe testing Si_3N_4, R = 50 nm	Friction coefficient in testing with a Si_3N_4 ball, R = 3 mm
Highly oriented pyrolytic graphite	0,09	0,006	0,1
Natural diamond	2,3	0,04	0,2
Single crystal Si (100)	0,14	0,07	0,4

appear in the middle of the last century. One of the first models of wear was developed by J. Archard [298], who used Holm's idea of [299] the adhesive seizure of interacting irregularities tops and transfer of the material from one asperity to another when destructing the bridge on the surface, which does not coincide with the initial contact border. From simple calculations it follows that the volume of the transferred material V is proportional to the normal force P_N and inversely proportional to the material hardness H in microasperities: $V = k_A P_N/H$. J. Archard model works well for friction pairs formed from the same relatively soft materials, such as annealed metals. In case of a pair of materials, which essentially differ from each other in hardness ($H_1 \geq 1{,}2H_2$), this model is improper because more solid asperities will simply cut off the soft ones. Nevertheless, in the model of E. Rabinovich [300], which takes this fact into account, the wear rate as in J. Archard model is proportional to P_N/H (but with a different coefficient – k_R): $V = k_R P_N/H$. Experience confirms this theoretical prediction for pure metals [301]. In the materials hardened by thermal treatment or cold-hardening there are deviations from the Rabinowich model, which is due to the transition to other wear modes. Thus, hardness and yield strength in small volumes (micro- or nano- depending on the extent of roughness) are the most important characteristics of the material exposed to wear. Of course, the transition to the nanoscale requires taking into account size effects, manifested, in particular, in the growth of hardness, flow stress and fracture.

Following the above said ideas, the hsrder is the material, the better it resists to wear. This is true for relatively soft materials, the hardness of which does not exceed a few GPa. However, for harder ($H \geq 10$ GPa) and superhard materials ($H \geq 30$ GPa) a combination of hardness H, Young's modulus E and fracture toughness K_{1c} is of crucial importance. In contrast to E, value H is quite sensitive to the size and structure of the deformation zone that is not explained exhaustively in nanoscale objects and requires special consideration. As noted above, data on the size dependence K_{1c} in nanoregion is virtually absent.

Express methods of attestation and prediction of wear resistance do not go beyond measuring H and K_{1C} of the material. Recently, however, several other criteria have been proposed, which are believed to more accurately reflect wear resistance: H/E, P_{Nc}^3/E^2, $\pi l \sigma_c^2/E$, here l is the length of the crack, σ_c is critical fracture stress, etc.

When asperities have a small size, on slippery surfaces there arises another scale effect, contributing to their strengthening – namely, rate. Indeed, the relative deformation rate $\dot{\varepsilon} \approx \Delta R/R\Delta t \approx v/R$ at a fixed linear rate v is inversely proportional to the characteristic size R of a deformable volume. Consequently, at quite moderate value $\upsilon = 1$ m/ s and $R \sim 10$–100 nm $\dot{\varepsilon}$ can reach values 10^7–10^8 s^{-1}, realized in macroexperiments upon detonation of the explosive on the sample surface. Under these conditions, material exhibits additional hardening several times as much.

Similar problems arise in the analysis of deformation, fracture, mechano-chemical synthesis and fusion, carried out in ball or jet mills, attritors and other process equipment designed for fine grinding of raw material. As the grinding of the initial components proceeds, particle size is reduced (up to a few tens of nanometers), and specific surface area increases up to hundreds m^2/g. This leads to a change in deformation and fracture mechanisms, acceleration of surface and volume diffusion, atomic mixing of the reactants which are not metallurgically miscible.

Practical applications and benefits of deep understanding and mastering triboproceses at the nanoscale are as diverse as their phenomenological manifestations. Here are the most attractive of them:

– building the basis of tribology from "the first principles";

– throwing bridges across all the scale levels of nanotribological processes consideration – from the atomic to the macroscopic, from the fundamental physical to the engineering;

– reduction of friction losses in mechanisms (ideally – to zero!);

– increase in wear resistance, friction coefficient in clutches, brakes, driving wheels in transport;

– the development of more effective MEMS/NEMS, data recording and storage systems, microrobot technique.

Nanomechanochemistry and nanomechanophysics

Mechanochemistry aims to study two classes of phenomena: the effect of mechanical stress on the chemism of substances, and vice versa – a change in the mechanical properties of solids as a result of chemical reactions in them [302–304]. Mechanophysics studies mechano-induced and cross-physical phenomena caused by a relationship between purely mechanical characteristics and electronic, magnetic, optical, emission and other responses. A detailed discussion of the peculiarities of mechanochemical and mechanophysical manifestations in the nanoscale is

beyond the scope of this review and deserves special consideration. We confine ourselves to listing and brief comments about some of them.

A systematic study of the processes that accompany cracking, crushing, attrition, fine grinding, intense shear deformation under pressure, etc. found out a large number of physical and chemical phenomena: the formation of free radicals and active centers, disordering, loosening and solids mechanolysis, emission of electrons, photons, ions and neutral atoms, the charging of fresh surfaces, acoustic emission, etc. [302]. On this basis there were developed technologies of mechanochemical synthesis of organic, inorganic and composite compounds, mechanical metals alloying (immiscible in metallurgical technologies), improving the quality of fillers for building materials and fuel coal.

A decrease in characteristic sizes to values at which atomic-molecular discreteness of an object and its quantum-mechanical behavior appear, blurs the boundaries between mechanics, physics and chemistry [17, 25, 32, 305]. In this scale it is necessary to take into account the possibility of local changes in the atomic and molecular structure of the object under the load, mechanostimulated chemical reactions, changes in the electron and phonon spectra (and hence the thermodynamic and kinetic characteristics of the substance), the emission of electrons, photons, ions and other particles. This greatly complicates the analysis of the behavior of nanoobjects in the field of mechanical stresses. On the other hand, only at this hierarchical scale level of solid structure one can understand the mechanisms of micro-alloying effect, mechanochemical reactions, dry friction and wear, light exposure, electromagnetic and ionizing radiation on the mechanical, physical and chemical properties of solids.

So, atomic mechanisms of deformation, diffusion and adhesion at the nanoscale determine the limiting particle sizes under heavy grinding, the possibility and kinetics of mechanochemical reactions in finely dispersed materials [302]. Fast processes in an electron-spin subsystem underlie the mechanisms of action of light exposure [306], weak ionizing radiation [307–309], electrical, magnetic and microwave fields [310–312] on the mechanical properties of solids. [313] describes active resonant influence of constant magnetic field and microwave magnetic field satisfying EPR conditions on dislocation mobility characteristics in nonmagnetic crystals. The reviews contained in [314, 315] summarize the results of weak magnetic fields effect on solid-state quasi-chemical reactions in the system of structural defects at the atomic scale and the mechanical properties of non-magnetic solids.

Mechanisms of protein synthesis, DNA replication, biochemical catalytic reactions involving enzymes are also dependent on the mechanical behavior of macromolecules, whose mechanical properties it has become possible to study in recent years. Biomechanics, molecular optoelectronics on rotaxane and catenane complexes also lies at the intersection of mechanics, physics and biochemistry [316, 317]. Thus, nanomechanics is becoming an integral part of physical chemistry, and in the field of nanosizes there takes place a natural convergence of many disciplines, which allows us to get better understanding of known phenomena and discover new ones.

Conclusion

Accumulated experimental data testify to considerable differences in the physico-mechanical properties of nominally the same material, but in the samples and structures with very different sizes of morphological elements or cross-section. This means that the size effects have a huge potential as a physical basis for the creation of high-performance materials from well-known raw materials. However, the nature of size effects in the physico-mechanical properties of advanced nanostructured materials, microsystem technology products, biomaterials needs to be systematically studied in the nanoscale. We emphasize that it is not reduced to a single mechanism even in a single material. Processes induced in a solid by mechanical action are complex and hierarchical, they can compete and either activate or limit each other. Multiscale physics of strength and plasticity of solids differentiates in polycrystalline materials at least 5 hierarchical scale levels – macro-, meso-, micro-, nano-, and atomic-electronic differing by patterns of behavior and character of size dependencies.

For the first three levels, there are approaches and theories that are in good agreement with experiments. As for the fourth and fifth levels, i.e. nanoscale and atomic-electronic ones, both experimental data and model representations about them are very scarce and often contradictory. We can only state the empirical fact: in many experiments materials in nanoscale exhibit shear strength and tensile strength close to their theoretical limits. As a consequence, under these conditions high values of hardness and wear resistance, low friction coefficient, and other anomalies in mechanical behavior are realized. Decoding the sequence of individual elementary events, the range of atomic defects taking part in them, the dynamics, the role and contribution of these defects in the plastic deformation, fracture, wear, mechanochemical transformations, mechanostimulated

physical phenomena need further investigation and clarification. Nanomechanical testing, alongside with other up-to-date methods of research, will be certainly extensively used to solve these important, both theoretical and applied problems.

Acknowledgements

This work was supported by the following grants: Russian Science Foundation (RSF) – grant № 15-19-00181 – nanoindentation technique and atomic models of local deformation, RSF – grant 14-13-00731 – technique and analysis of single-molecule force spectroscopy, the Ministry of Education and Science of RF – K1-2014-022 (theory and calculations of mechanical properties and dynamics of macromolecules).

References

221. J. Li, K.J. Van Vliet, T. Zhu, S. Yip, S. Suresh. *Nature*, 418, 307 (2002)

222. K.J. Van Vliet, J. Li, T. Zhu, S. Yip, S. Suresh. *Phys. Rev. B.*, 67, 104105-1 (2003)

223. C.A. Schuh, A.C. Lund. *J. Mater. Res.*, 19, 2152 (2004)

224. D. Lorenz, A. Zeckzer, U. Hilbert, P. Grau, H. Johansen, H.S. Leipner. *Phys. Rev. B.*, B67, 172101 (2003)

225. A.M. Minor, E.T. Lilleodden, E.A. Stach, J.W. Morris. *J. Mater. Res.*, 19, 176 (2004)

226. M. Jin, A.M. Minor, E.A. Stach, J.W.Jr. Morris. *Acta. Mater.*, 52, 5381 (2004)

227. M. Jin, A.M. Minor, J.W.Jr. Morris. *J. Mater. Res.*, 20, 1735 (2005)

228. Yu.I. Golovin, A.I. Tyurin, B.Ya. Farber. *J. Mater. Sci.*, 37, 895 (2002)

229. Yu.I. Golovin, A.I. Tyurin, B.Ya. Farber. *Phil. Mag. A.*, 82, 1857 (2002)

230. Yu.I. Golovin, V.I. Ivolgin, V.V. Korenkov, A.I. Tyurin, B.Ya. Farber. *Materials Science Forum,* 386–388, 141 (2002)

231. C.A. Schuh, J.K. Mason, A.C. Lund. *Nature Materials*, 4, 617 (2005)

232. H. Li, A.H.W. Ngan, M.G. Wang. *J. Mater. Res.*, 20, 3072 (2005)

233. J.K. Mason, A.C. Lund, C.A. Schuh. *Phys. Rev. B.*, B73, 054102-1 (2006)

234. C.E. Packard, C.A. Schuh. *Acta Mater.*, 55, 5348 (2007)

235. A. Gouldstone, N. Chollacoop, M. Dao, J. Li, A.M. Minor, Y-L. Shen. *Acta Mater.*, 55, 4015 (2007)

236. M.S. Bodji, J.B. Pethica, B.J. Inkson. *J. Mater. Res.*, 20, 2726 (2005)

237. Yu.I. Golovin, A.I. Tyurin. *JETP Letters*, 60, 742 (1994)

238. Yu.I. Golovin, A.I. Tyurin. *Physics of the Solid State,* 38 (6), 1000 (1996)

239. Yu.I. Golovin, A.I. Tyurin. *Crystallography reports (Russia)*, 40, 884 (1995)

240. Yu.I. Golovin, A.I. Tyurin, V.Z. Bengus, V.I. Ivolgin, V.V. Korenkov. *Physics of Metals and Metallography*, 88 (6), 612 (1999)

241. Yu.I. Golovin, V.I. Ivolgin, V.V. Korenkov, A.I. Tyurin. *Physics of the Solid State*, 39 (2), 278 (1997)

242. Yu.I. Golovin, A.I. Tyurin. *Physics of the Solid State,* 42 (10), 1865 (2000)

243. Yu.I. Golovin, A.I. Tyurin, V.I. Ivolgin, V.V. Korenkov. *Technical Physics*, 45 (5), 605 (2000)

244. Manika, J Maniks. *Acta Mater.*, 54, 2049 (2006)

245. J.W.C. Dunlop, R. Weinkamer, P. Fratzl. *Materials Today*, 14, 70 (2011)

246. Meyers, P.-Y. Chen, A.Y.-M. Lin, Y. Seki. *Progr. Mater. Sci.*, 53, 1 (2008)

247. J. Aizenberg, P. Fratzl. *Adv. Mater.*, 21, 387 (2009)

248. P. Fratzl, F.G. Barth. *Nature*, 462, 442 (2009)

249. M.J. Buehler. *Nano Today*, 5, 379 (2010)

250. F.J. O'Brein. *Materials Today*, 14, 88 (2011)

251. R. Akhtar, M.J. Sherratt, J.K. Cruickshank, B. Derby. *Materials Today,* 14, 96 (2011)

252. Zamari, S. De. *J. of Mech. Behavior of Biomedical Mater.*, 4, 146 (2011)

253. S. Pathak, J.G. Swadener, S.R. Kalidindi, H.-W. Courtland, K.J. Jepsen, H.M. Goldman. *J. of Mech. Behavior of Biomedical Mater.*, 4, 34 (2011)

254. D. Lahiri, V. Singh, A.P. Benaduce, S. Seal, L. Kos. *J. of Mech. Behavior of Biomedical Mater.*, 4, 44 (2011)

255. J. Burket, S. Gourion-Arsiquaud, L.M. Havill, S.P. Baker, A.L. Boskey, M.C. van der Meulen. *J Biomech.*, 44(2), 277-84 (2011).

256. N. Martin, A. Garcia, V. Vera, M.A. Garrido, J. Rodríguez. *Am. J. Dent.*, 23(2), 108-12 (2010).

257. G. Lewis, J.S. Nyman. *J. Biomed. Mater. Res. B Appl. Biomater.,* 87(1), 286-301 (2008).

258. R. Akhtar, N. Schwarzer, M.J. Sherratt, R. Watson, H. Graham, A. Trafford, P. Mummery, B. Derby. *J. Mater. Res.*, 24(3), 638-646 (2009)

259. M.R. Ahmad, M. Nakajima, S. Kojima, M. Homma, T. Fukuda. *IEEE Trans. Nanobioscience,* 9 (1), 12-23 (2010)

260. P.S. Wo, L. Zuo, A.H.W. Ngan. *J. Mater. Res.*, 20, 489 (2005)

261. Yu.I. Golovin, S.N. Dub, V.I. Ivolgin, V.V. Korenkov, A.I. Tyurin. *Physics of the Solid State*, 47 (6), 995 (2005)

262. B.S. Bokshteyn, A.B. Yaroslavtsev. *Diffuziya atomov i ionov v tverdyih telah (Atoms and ions diffusion in solids).* Izd-vo MISIS, Moskva, 2005. S. 362 (Rus)

263. V.L. Indenbom. *JETP Letters*, 12 (11), 369 (1970)

264. V.N. Rozhanskii, M.P. Nazarova, I.L. Svetlov, L.K. Kalashnikova. *Phys. Stat. Sol. A.*, 41, 579 (1970)

265. T. Zhu, J. Li, K.J. VanVliet, S. Ogata, S. Yip, S. Suresh. *J. Mech. Phys. Solids*, 52, 691 (2004)

266. Szlufarska. *Materials Today*, 9, 42 (2006)

267. J.R. Greer, W.D. Nix. *Phys. Rev. B.*, B73, 245410-1 (2006)

268. M.A. Begley, J.W. Hatchinson. *J. Mech. Phys. Solids*, 46, 2049 (1998)

269. W.D. Nix, H. Gao. *J. Mech. Phys. Solids*, 46, 411 (1998)

270. *Handbook of Nanostructured Materials and Nanotechnology*. (Ed. H.S. Nalwa). 1-5. Academic Press. San Diego. 1999.

271. K. Chen, W.J. Meng, F. Mei, J. Hiller, D.J. Miller. *Acta Mater.*, 59, 1112 (2011)

272. S. Qu, Y. Huang, W.D Nix., H. Jiang, F. Zhang, K.C. *J. Mater. Res*., 19, 3423 (2004)

273. N.A. Fleck, J.W. Hatchinson. *J. Mech. Phys. Solids*, 41, 1825 (1993)

274. V. Domnich, Y. Gogotsi. *Rev. Adv. Mater. Sci.*, 3, 1 (2002)

275. J.-J Kim., Y. Cyoi, S. Suresh, A.S. Argon. *Science*, 295, 654 (2002)

276. Y.G. Gogotsi, A. Kailer, K.J. Nickel. *Nature*, 401, 663 (1999)

277. R.H.J. Hannik, P.M. Kelly, B.C. Muddle. *J. Am. Ceram. Soc*., 83, 461 (2000)

278. C. Piconi, G Maccauro. *Biomaterials*, 20, 1 (1999)

279. Yu. Gogotsi., V. Domnich, S.N. Dub, A. Kailer, K.G. Nicckel. *J. Mater. Res*., 15, 871 (2000)

280. Yu.I. Golovin, V.I. Ivolgin, V.V. Korenkov, B.Ya. Farber. *Physics of the Solid State*, 43, 2105 (2001)

281. V.Z. Parton, E.M. Morozov. *Mehanika uprugoplasticheskogo razrusheniya (Mechanics of elastic-plastic fracture)*. Izd-vo Mashinostroenie, Moskva, 1985.504 s. (Rus)

282. V.M. Pestrikov, E.M. Morozov. *Mehanika razrusheniya tverdyih tel (Mechanics of fracture in solids)*. Izd-vo Mashinostroenie, Moskva, 2002. 320 s. (Rus)

283. GOST 25.506-85. Raschetyi i ispyitaniya na prochnost. Metodyi mehanicheskih ispyitaniy metallov. Opredelenie harakteristik treschinostoykosti (vyazkosti razrusheniya) pri staticheskom nagruzhenii (*Design, calculation and strength testing. Method of mechanical testing of metals. Determination of fracture toughness characteristics under the statistic loading*.) Izd-vo standartov, Moskva. 61 (1985) (Rus)

284. T. Nose, T. Fujii. *J. Am. Ceram. Soc*., 71, 328 (1988)

285. T. Hansson, R. Warren, J. Wasen. *J. Am. Ceram. Soc*., 76, 841 (1993)

286. J. Gong. *Ceram. Intern*., 28, 767 (2002)

287. J. Wang, J. Gong, Z. Guan. *Mater. Lett*., 57, 643 (2002)

288. Y. Charles, D. Vandembroucq, F. Hild, S. Roux. *J. Mech. Phys. Solids*, 52, 1651 (2004)

289. Y. Charles, F. Hild, S. Roux, D. Vandembroucq. *Int. J. Fract*., 142, 51 (2006)

290. H. Miyazaki, H. Hynga, K. Hirao, T. Ohji. *J. Eur. Ceram*. Soc., 27, 2347 (2007)

291. W. Weibull. *Royal Sweden Inst. Eng. Res*., 151, 121 (1939)

292. C.B. Ponton, R.D. Rawlings. *Mater. Sci. Technol*., 5, 865 (1989)

293. C.B. Ponton, R.D. Rawlings. *Mater. Sci. Technol*., 5, 961 (1989)

294. M. Sakai, R.C. Bradt. *Inter. Mater. Rev*. 38, 53 (1993)

295. D.S. Harding, W.C. Oliver, G.M. Pharr. *MRS Symp. Proc*., 356, 663 (1995)

296. A.G. Evans, E.A. Charles. *J. Am. Ceram. Soc*., 59, 371 (1976)

297. *Fundamental of Friction*. (Ed. B. Bhushau). Berlin. Springer, 2008. 356 p.

298. J.F. Archard. *Journal of Applied Physics*. 24, 981 (1953)

299. K. Holm. *Electrical contacts*. H. Gerber Publ, Stockholm, 1946. 256 p.

300. E. Rabinovicz. *Friction and wear of materials*. Wiley and Sons, Weinheim, 1965. 384 p.

301. M.M. Hruschev, M.A. Babichev. *Issledovanie iznashivaniya materialov (The study of materials wear)*. Izd-vo Nauka, Moskva, 1970. 315 s. (Rus)

302. *Fundamentalnyie osnovyi mehanicheskoy aktivatsii, mehanosinteza i mehanohimicheskih tehnologiy (Fundamentals of mechanical activation, mechanical synthesis and mechanochemical technology)* (pod red. E.G. Avvakumova). Izd-vo SO RAN, Novosibirsk, 2009. 342 s. (Rus)

303. V.V. Zyryanov. *Russian Chemical Reviews*, 77, 105 (2008)

304. N.Z Lyakhov, T.F. Grigorieva, A.P. Barinova, I.A. Vorsina. *Russian Chemical Reviews*, 79, 189 (2010)

305. A.L. Buchachenko. *Russian Chemical Reviews*, 72, 375 (2003)

306. Yu. A. Osip'yan. *Adv. Phys*. 35, 115 (1986)

307. J.H. Ke, T.L. Yang, Y.S. Lai, C.R. Kao. *Acta Mater*., 59, 2462 (2011)

308. N.A. Jamal, H. Anuar, A.R.S. Bahri. *J. Nanotechnology*. (2011). Article ID 683725. Doi: 101155/2011/683725

309. A.A. Dmitrievskii, N.Yu. Efremova, Yu.I. Golovin, A.V. Shuklinov. *Journal of Surface Investigation. X-ray, Synchrotron and Neutron Techniques*, 4, 229 (2010)

310. B. Malard, J. Pilch, P. Sittner, R. Delville, C. Curfs. *Acta Mater*., 59, 1542 (2011)

311. Yu.I. Golovin. *Magnitoplastichnost tverdyih tel (Magetic plasticity of solids*). Mashinostroenie, Moskva, 2003. 108 s. (Rus)

312. *Magneto-Science. Magnetic Field Effects on Materials: Fundamental and Application* (Ed. M. Yamaguchi, Y. Tanimoto). Kodansha Ltd, Tokyo, Springer, Berlin, Heidelberg, New York. 2006. 354 p.

313. Y. Golovin, R. Morgunov, A. Baskakov. *Molecular Physics*, 100, 1291 (2002)

314. Yu.I. Golovin. *Physics of the Solid State* 46 (5), 789 (2004)

315. V.I. Alshits, E.V. Darinskaya, M.V. Koldaeva, E.A. Petrzhik. In *Dislocation in Solids. V. 14*. (Ed. J.P. Hirth). Elsevier, Amsterdam. 2008. p. 333

316. V. Balzani, M. Venturi, A. Credi. *Molecular Devices and Machines. Concepts and Perspectives for the Nanoworld.* Wiley-VCH, Weinheim. 2008. 552 p.

317. V.A. Karasev, V.V. Luchinin. *Vvedenie v konstruirovanie bionicheskih nanosistem (Introduction to the design of bionic nanosystems*). FIZMATLIT, Moskva, 2009. 464 p. (Rus)